POLITECNICO
MILANO 1863

SCUOLA DI INGEGNERIA INDUSTRIALE
E DELL'INFORMAZIONE

Executive Summary of the Thesis

# Multi-input Lateral Dynamics Control of an Electric Vehicle

Laurea Magistrale in Mechanical Engineering - Ingegneria Meccanica

**Author:** Divy Dhingra

**Advisor:** Dr. Michele Vignati

**Co-advisors:** Ing. Michele Asperti, Prof. Edoardo Sabbioni

**Academic year:** 2020-2021

## 1. Introduction

The aim of this thesis is to develop a multi-input multi-output (MIMO) controller for improving vehicle lateral dynamics. Rear steering and torque vectoring are used as active systems. For commercial vehicles, a fast, simple and stable controller is desirable for running in real time during any maneuver. The controller should be able to handle the nonlinearity of lateral dynamics without increasing the computational cost or design complexity.
First, transfer functions are derived for the linearised single track model (LSTM) of a vehicle with active rear steering and torque vectoring. The effect of rear steering and torque vectoring on vehicle lateral dynamics is first studied by evaluating step response and frequency response of transfer functions.
A couple of controllers has been tested: a feedforward controller and an integral terminal sliding mode controller (ITSMC). A method of calculating the reference yaw rate and sideslip angle values using a logistic function is also presented. Both the controllers are first tested using LSTM. These controllers are then tested by performing steady state and transient maneuvers using the more realistic VI-CarRealTime (VI-CRT) model.
ITSMC relies on real time knowledge of vehicle sideslip angle. The sideslip angle cannot be directly measured in commercial vehicles using cost-effective sensors. Moreover, sliding mode controllers are known to suffer from undesirable finite amplitude oscillations, known as chattering, in system response due to unmodelled dynamics.
An asymptotic state observer can avoid such chattering in the system reponse. Thus, an extended Kalman filter is used as the observer to estimate vehicle sideslip angle, filter the noisy yaw rate signal and also avoid chattering. The ITSMC controller with EKF is then compared with another sliding mode controller from literature.

## 2. Active Rear Steering and Torque Vectoring

The forces, moments, velocities and inertial accelerations acting on the vehicle under the assumptions of single track model are presented in Figure 1. The linearised equations of motion for the vehicle in curve in matrix notation as follows:

$$\dot{\underline{z}} = [A]\underline{z} + [C]\delta_F + [B]\underline{u},\ \underline{u} = [\delta_r, M_z]^T \quad (1)$$

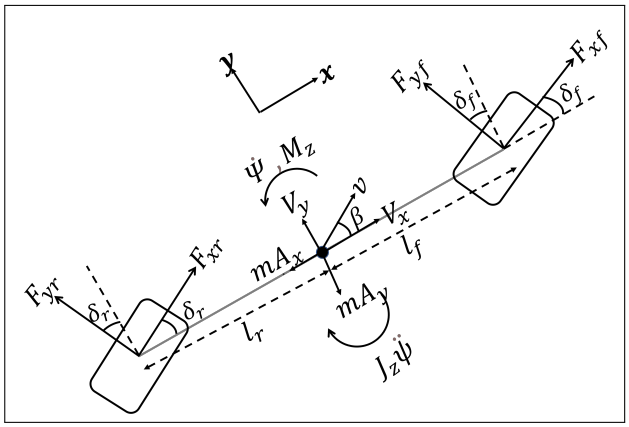


Figure 1: Single Track Model (STM) of a vehicle in curve with ARS and TV.

where $\underline{z} = [\dot{\psi}, \beta]^T$ is the state vector, $\dot{\psi}$ is vehicle yaw rate and $\beta$ is vehicle sideslip angle. The transfer functions relating the two model outputs $\dot{\psi}$ and $\beta$ to the model inputs $\delta_f$ and $M_z$ for the above system of equations are calculated after substituting $\delta_r = K_w \delta_f$. Thus, a negative $K_w$ would imply that rear wheels are steered in the opposite direction to front wheels.

The rear-to-front steering ratio ($K_w$) affects only the transfer functions relating model outputs to $\delta_f$. The frequency response functions (FRF) and step response are evaluated for 4 different values of $K_w$ $(-1, -1/3, 1/3, 1)$ and 2 different speeds (10 $km/h$ and 90 $km/h$). The frequency response function (FRF) for $\dot{\psi}$ increases with the magnitude of negative $K_w$ at both vehicle speeds (Figures 2 and 3). The magnitude of FRF for $\beta$ is lower for negative $K_w$ at low vehicle speed. At high vehicle speed, the FRF for $\beta$ may be lower for a positive $K_w$ depending on the excitation frequency.

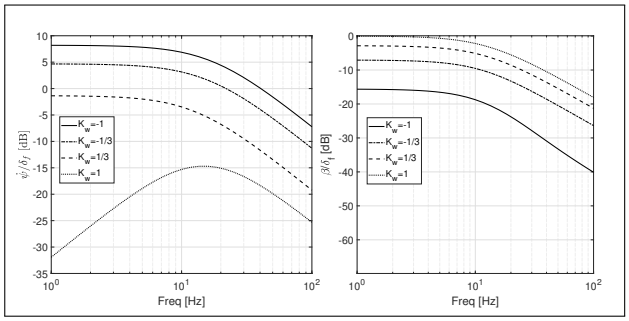


Figure 2: Effect of $K_w$ on FRFs at 10 $km/h$.

Thus, if the vehicle speed is low, a higher $\dot{\psi}$ can be achieved with respect to passive vehicle while also minimizing $\beta$ by steering the rear wheels in the direction opposite to front wheels. At higher vehicle speed, increasing yaw rate by counter steering the rear wheels may considerably increase the magnitude of $\beta$, especially during low frequency excitations of $\delta_f$. Such an increase may result in unstable behaviour of the vehicle due to high slip angles at the wheels. These observations are further verified by analysing the step response of the relevant transfer functions. Next we analyse the effect of yaw moment $M_z$ on vehicle lateral dynamics. We calculate the frequency response functions and step response of the transfer functions for vehicle speeds of 10 $km/h$ and 90 $km/h$. The transfer functions relating model outputs ($\dot{\psi}$ and $\beta$) with $M_z$ are not affected by $K_w$.

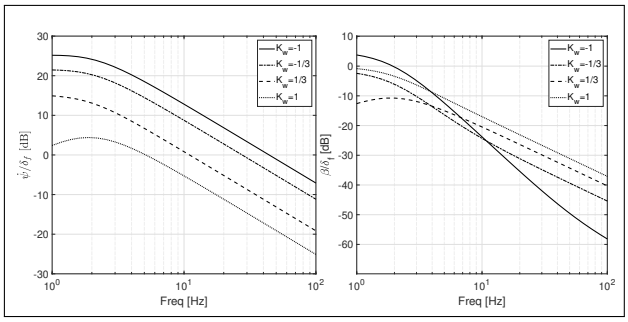


Figure 3: Effect of $K_w$ on FRFs at 90 $km/h$.

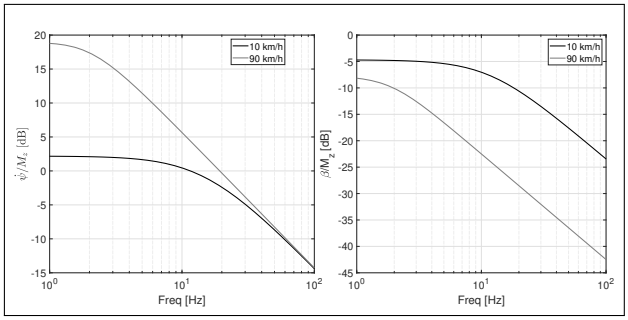


Figure 4: Effect of vehicle speed on FRFs for $M_z$.

The magnitude of the FRF increases with vehicle speed for both $\dot{\psi}$ and $\beta$ for excitation frequencies lower than 10 $Hz$ (Figure 4). At higher excitation frequency, the FRF for low vehicle speed is higher. Also, the steady state value of $\beta$ is lower than that of $\dot{\psi}$. Thus, for same $M_z$, the gain for $\dot{\psi}$ will always be higher than that for $\beta$. Based on the observations drawn from evaluating the transfer functions, we can conclude that a combination of active rear steering and torque vectoring can obtain desired yaw rate while min-

imizing sideslip angle, especially at high speed. At high speed, we need to implement positive $K_w$ in order to reduce $\beta$. This would reduce the steady state value for $\dot{\psi}$. The yaw moment generated by TV can increase the yaw rate steady state value without significantly affecting the steady state value of $\beta$. Hence, a combination of the two inputs becomes necessary to achieve the target $\beta$ and $\dot{\psi}$, particularly at high speed.

## 3. Controllers

In this section, an integral terminal sliding mode controller is presented. A method for calculating reference values using logistic function is also presented. The extended Kalman filter used in this thesis is also presented.

### 3.1. Integral Terminal Sliding Mode Controller

The integral terminal sliding mode control (ITSMC) is a feedback controller. The sliding surfaces are defined as:

$$\underline{\mathrm{S}} = [K_e] \begin{bmatrix} a(e_{I,\dot{\psi}})^p + b(e_{I,\dot{\psi}})^g + (\dot{\psi}_r - \dot{\psi}) \\ a(e_{I,\beta})^p + b(e_{I,\beta})^g + (\beta_r - \beta) \end{bmatrix}, \quad (2)$$

where $e_{I,\dot{\psi}} = \int_0^t (\dot{\psi}_r - \dot{\psi}) d\tau$, $e_{I,\beta} = \int_0^t (\beta_r - \beta) d\tau$ and $[K_e]$ is a $2 \times 2$ constant non-singular matrix. Here, $1 < p < 2$, $g > p$ and $b \geq a$. Such a definition of sliding surfaces ensures that the convergence rate stays reasonably high even when we get close to the reference values. The controller inputs are derived by imposing the following condition for surface reachability:

$$\dot{\underline{\mathrm{S}}} = -\begin{bmatrix} \frac{K_1 S_1}{|S_1| + K_3} \\ \frac{K_2 S_2}{|S_2| + K_4} \end{bmatrix}, \quad (3)$$

where $K_1$, $K_2$, $K_3$ and $K_4$ are positive constants and $S_1$ and $S_2$ are the elements of $\underline{\mathrm{S}}$. This helps in avoiding the chattering due to finite sampling rate and ensures that $\underline{\mathrm{S}}^T \dot{\underline{\mathrm{S}}} < 0$, which is essential for stability and convergence to the sliding surfaces.

### 3.2. Reference $\dot{\psi}_r$ and $\beta_r$

The reference yaw rate ($\dot{\psi}_r$) is calculated as:

$$\dot{\psi}_r = \frac{K}{1 + e^{-r'\delta_{SW}}} - 0.5K, \; r' = \frac{\eta_{\dot{\psi}} h v}{l(1 + kv^2)}, \quad (4)$$

where $k$ is the understeering coefficient, $\eta_{\dot{\psi}}$ is the desired scaling factor for yaw rate and $K$ and $h$ are obtained by fitting the above equation (with $\eta_{\dot{\psi}} = 1$) to passive vehicle's steering wheel angle-yaw rate curve. In this thesis, $\eta_{\dot{\psi}} = 1.1$ to achieve 10% improvement in yaw rate of passive vehicle.

The reference sideslip angle ($\beta_r$) is calculated as:

$$\beta_r = \begin{cases} F\eta_\beta \dot{\psi}_{pas} & F > 0 \\ F(2 - \eta_\beta)\dot{\psi}_{pas} & F \leq 0 \end{cases}, \quad (5)$$

$$F = \left( \frac{l_r}{v} - \frac{m l_f v}{l K_r} \right) \quad (6)$$

where $\dot{\psi}_{pas}$ is calculated using Equation 4 with $\eta_{\dot{\psi}} = 1$. In this thesis, $\eta_\beta = 0.5$ to achieve 50% scaling of passive vehicle's $\beta$. If $\beta_r = 0$, the actuator inputs are quite high as compared to $\beta_r \neq 0$ and calculated using the above equation. This reduction in actuator inputs is helpful especially when they are undersized.

### 3.3. Extended Kalman Fiter

The EKF uses the nonlinear lateral dynamics model. The lateral forces are calculated using the nonlinear three parameter Pacejka tyre model:

$$F_{yj} = D_j \sin[C_j \arctan(B_j \alpha_j)], \quad (7)$$

$$_j = \mu F_{zj} d_j, \; B_j = \frac{b_j}{\mu}, \; j = f, r, \quad (8)$$

where $\mu$ is the friction coefficient. Here, the parameters $C_j$, $d_j$ and $b_j$ are calculated by fitting the above equation to the normalised lateral force-average lateral slip curves generated by steady state ramp steer maneuver at 90 $km/h$.

The calculation of lateral forces requires the knowledge of friction coefficient between tyre and road surface. This also cannot be measured directly and is estimated by the EKF. The augmented state vector then becomes:

$$\underline{\mathrm{z}} = \begin{bmatrix} \underline{\mathrm{x}} \\ \mu \end{bmatrix} = \begin{bmatrix} v_y \\ \dot{\psi} \\ \mu \end{bmatrix}, \quad (9)$$

where $\underline{\mathrm{x}}$ is the state vector of the system.

A lot of vehicles equipped with the Electronic Stability Controller (ESC) use sensors that measure yaw rate ($\dot{\psi}$) and lateral acceleration ($a_Y$).

Thus, the EKF uses these quantities for constructing a measurement vector at each step.
The EKF estimates $\beta$ and filters the noisy signal of $\dot{\psi}$. These quantities are passed to the integral terminal sliding mode controller (ITSMC) to calculate the actuator inputs. The calculated inputs are then forwarded to the VI-CRT model which simulates vehicle dynamics and generates the clean signals for $\dot{\psi}$, $a_y$ and other quantities. The noise is added to these clean signals before passing them to the EKF for estimation.

## 4. Simulation Results

The simulation results obtained using the VI-CRT `CityCar_FullElectric` model are presented in this section. The `CityCar_FullElectric` model is originally defined as a front wheel drive (FWD) vehicle with front steering only. For the purpose of this work, a rear steering system kinematically equivalent to front one is added to the VI-CRT model.
The FWD powertrain is substituted with an equivalent 4 in-wheel motors (IWMs) powertrain. The mechanical characteristics of the 4 IWMs are calculated such that the new powertrain is equivalent to the FWD system in terms of the total torque generated at the wheels. A lower level controller which converts the required yaw moment into driving or braking torque applied to the wheels while accounting for friction or actuator limits is also designed. Equal magnitude and opposite sign of driving moments are applied to the left and the right wheel of each axle to generate an additional yaw moment ($M_z$). This allows the vehicle to maintain its speed during the maneuver.

### 4.1. Integral Terminal Sliding Mode Controller

The controller parameters are tuned using trial-and-error method. The derivation of controller inputs using LSTM generates a feedforward (FF) type contribution to the inputs. During the simulations with VI-CRT model, this FF type contribution results in abrupt peaks in system response. To generate a smoother response, the FF type part for actuator input calculation is removed.
The results for steady state high speed ramp steer maneuver are presented in Figure 5. The controller is able to track the reference yaw rate close to the friction limit. The controller is able to track the reference $\beta_r$ up to 200 $s$, after which the $|\beta|$ of active vehicle is still lower than that of the passive vehicle.

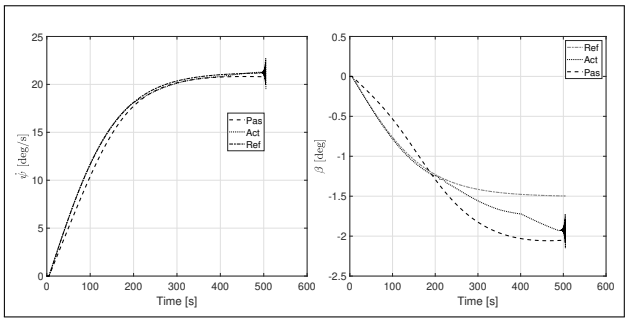


Figure 5: High speed (25 $m/s$) ramp steer maneuver for 10% improvement in $\dot{\psi}$ using ITSMC.

The results for high speed step steer maneuver are presented in Figure 6. The controller converges to the reference yaw rate within 1 $s$ from the starting of the maneuver, with almost no oscillations thereafter. Thus improving the yaw rate of the active vehicle by 10% as compared to the passive vehicle without significantly increasing the vehicle sideslip angle. The convergence rate is found to be slower during the low speed ramp steer maneuver.

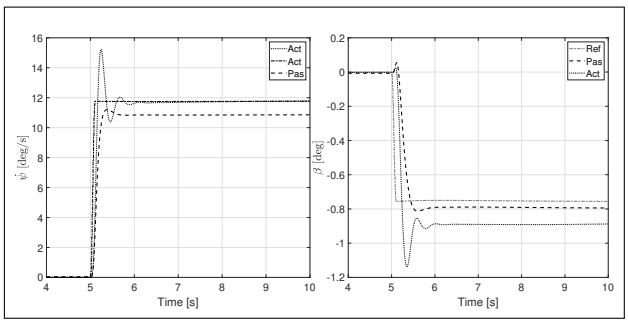


Figure 6: High speed (25 $m/s$) step steer maneuver with 10% improvement in $\dot{\psi}$ using ITSMC.

### 4.2. Observer in the Loop

As discussed before, ITSMC relies on real time knowledge of vehicle sideslip angle which cannot be directly measured in a real vehicle. In this thesis, an extended Kalman filter (EKF) is used to estimate $\beta$, filter noisy yaw rate signal and avoid any chattering due to unmodelled dynamics. The controller parameters had to be retuned after adding EKF to the control loop as

some undesired oscillations in system response are observed during high speed ramp steer maneuver.

The results of high speed ramp steer maneuver are presented in Figure 7. The controller with EKF is able to track the reference yaw rate even during very high lateral acceleration (close to the friction limit). At high lateral acceleration, some estimation error in sideslip angle can be observed. However, this does not affect yaw rate tracking drastically. For low lateral accelerations, the friction coefficient estimation is found to be poor. This is mainly because friction coefficient is non-observable when the lateral acceleration is extremely low.

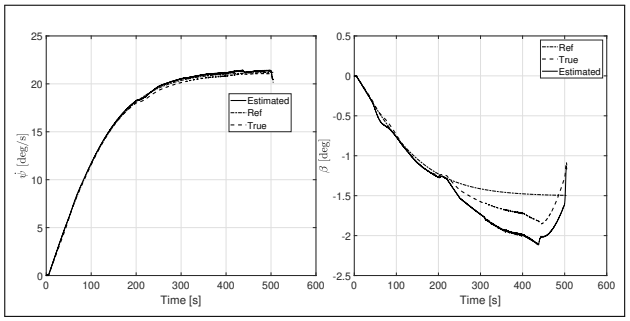


Figure 7: High speed (25 $m/s$) ramp steer maneuver using ITSMC with EKF added to the loop.

The non-observability of friction coefficient results in large estimation errors in yaw rate and sideslip angle during the low speed ramp steer maneuver. The controller is able to maintain the estimated values close to the reference signals. At low speed, the vehicle dynamics is slow and stable. The system response qualitatively similar to that of passive vehicle. Thus, the driver may not be required to make abrupt steering changes during low lateral acceleration maneuvers.

The high speed step steer maneuver results are presented in Figure 8. The convergence rate of the controller with EKF is found to be slower than the controller without EKF. The convergence is even slower when the vehicle speed is low. The controller with EKF generates lower over shoots as compared to the controller without EKF. This can also be because of different parameters used for the controller with EKF.

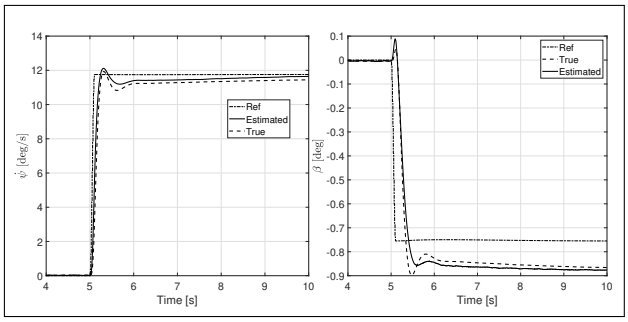


Figure 8: High speed (25 $m/s$) step steer maneuver using ITSMC with EKF added to the loop.

## 4.3. Comparison with a controller from literature

A sliding mode controller from literature is compared with ITSMC (with EKF). The controller from literature does not have any integral terms in the defintion of its sliding surfaces. We implement this controller by switching off the integral terms of the ITSMC derived in this thesis. The controller from literature is tuned such that the controller gains are as high as possible while generating smooth system response, especially for high speed ramp steer maneuver.

The high speed ramp steer maneuver results are presented in Figure 9. Here, the actuator inputs and true signals of yaw rate and sideslip angle generated by the two controllers are compared. In Figure 9, it can be observed that the ITSMC (with EKF) tracks the reference yaw rate signal better than the controller from literature. The magnitude of sideslip angle of ITSMC is also lower as compared to the controller from literature.

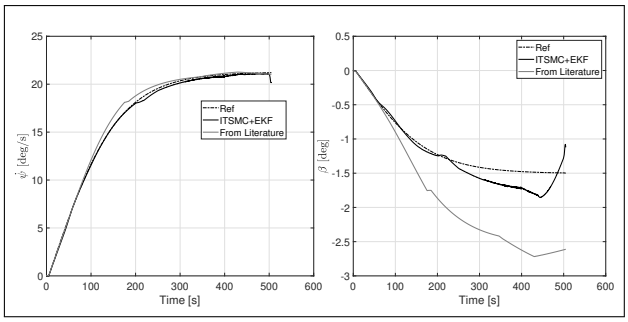


Figure 9: Comparison between a controller from literature and ITSMC with EKF for high speed (25 $m/s$) ramp steer maneuver.

The two controllers perform similar during the

step steer maneuvers as shown in Figure 10. Th ITSMC appears to be converging to the reference signals whereas the controller from literature appears to have achieved a steady state value.

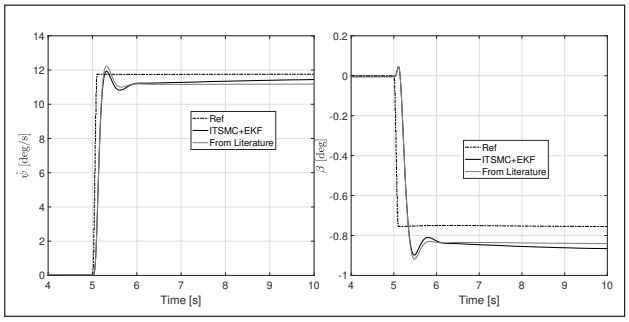


Figure 10: Comparison between a controller from literature and ITSMC with EKF for high speed (25 $m/s$) step steer maneuver.

## 5. Bibliography

The integral terminal sliding mode controller is developed following the approach presented in [1–3]. The EKF used in this thesis work is presented and discussed in [4, 5].

## 6. Conclusions

In this thesis, a multi-input multi-output (MIMO) controller for improving vehicle lateral dynamics has been developed. The actuator inputs when $\beta_r = 0$ are significantly higher when compared to $\beta_r$ closer to the passive one. A new method for generating yaw rate and sideslip angle reference signals is also explored. The integral terminal sliding mode controller (ITSMC), being a feedback controller, can track the reference yaw rate while achieving less than desired improvement on sideslip angle. The ITSMC prioritises yaw rate tracking due to particular tuning of controller parameters.

An extended Kalman filter (EKF) is used to estimate vehicle sideslip angle in real time using the data from available on-board sensors. The EKF is able to estimate sideslip angle with reasonable accuracy for moderate to high lateral accelerations in real time. The filter convergence is found to be poor for low lateral accelerations where friction coefficient is non-observable.

The ITSMC with EKF is then compared with another sliding mode controller from literature, which does not use integral terminal terms in sliding surface definition. The ITSMC tracked yaw rate better than the existing controller and also resulted in better sideslip angle response as compared to the existing controller.

## 7. Acknowledgements

I am extremely grateful to Prof. Michele Vignati for giving me the opportunity to work on this beautiful and challenging problem. I would like to thank Ing. Michele Asperti for his valuable inputs during discussions and writing of this thesis.

## References

[1] Josef Zehetner and Martin Horn. Vehicle dynamics control with torque vectoring and active rear steering using sliding mode control. *IFAC Proceedings Volumes*, 40(10):1–8, 2007.

[2] Lei Qiao and Weidong Zhang. Trajectory tracking control of auvs via adaptive fast nonsingular integral terminal sliding mode control. *IEEE Transactions on Industrial Informatics*, 16(2):1248–1258, 2020. doi: 10.1109/TII.2019.2949007.

[3] Heide Brandtstädter. *Sliding Mode Control of Electromechanical Systems*. Dissertation, Technische Universität München, München, 2009.

[4] Michele Vignati, Edoardo Sabbioni, and Davide Tarsitano. Torque vectoring control for iwm vehicles. *International Journal of Vehicle Performance*, 2(3):302–324, 2016.

[5] Michele Vignati. *Innovative control strategies for 4WD hybrid and electric control*. PhD thesis, Politecnico di Milano, Italy, 1 2017.